Egyptian Geophysical Society
EGS Journal, vol. 3, No. 1, 17-26 (2005)

RESERVOIR ROCK PROPERTIES OF THE MIDDLE FRIO FORMATION (DEEPER F-SERIES), STRATTON FIELD, SOUTH TEXAS, USA

Hamed Zeidan El-Mowafy

Department of Geology, Faculty of Science, Al-Azhar University, Nasr City, Cairo, Egypt

خواص الصخر الخازن لتكوين فريو المتوسط (سلسلة – اف العميقة)، حقل ستراتون،

جنوب تكساس، الولايات المتحدة الأمريكية

الخلاصة: ينتج حقل ستراتون فى جنوب تكساس من طبقات حجر رملى متعدده مبعثرة ومركزة تحتوى على الهيدروكربون فى تكوين فريو الاوليجوسينى. ويعتبر تكوين فريو المتوسط أهم خزان للغاز فى منطقه ساحل خليج تكساس. ولفهم أفضل لاستغلال واستكشاف هذا الخزان فإنه من المهم تحديد خواصه الفيزيائية الصخرية لكى تربط بالملاحظات السيزمية مثل السعة وزمن الإرتحال. وفى هذا البحث تم حساب الكثافة ومعامل الانضغاطية وسرعة الموجات الصوتية لخزان فريو المتوسط المكون من الحجر الرملى النقى فى حقل ستراتون. كما تم تحديد الثوابت الاختبارية " المعاملات الحرة " إحصائيا من السرعة الصوتية الملاحظة والمسامية. كما استخدمت قيم معاملات أفضل تناسب لحساب معامل الإطار الصخرى المسامى الجاف والتى بالتالى استخدمت لحساب معامل المستوى الموجى المشبع والسرعة لإطار الصخرالمسامى المشبع. كما تم التنبؤ بالتغيرات فى معاملات صخر فريو المتوسط بواسطة التغيرات فى معامل الانعكاس المحسوب على قمة خزان فريو المتوسط. كما لوحظ أن إضافة الغاز انقصت بشدة كثافة وسرعة الموجات الصوتية داخل الصخر ونتج عنها معامل انعكاس سلبى "نطاق متأثر بنقطة قاتمة".

ABSTRACT: *Stratton field in south Texas produces from multiple dispersed and concentrated sandstone pays in the Oligocene Frio Formation. The middle Frio Formation is the most important gas reservoir in the Frio Reservoir gas play in the Texas Gulf Coast region. For better understanding of exploitation and exploration of this reservoir it is important to determine its rock physics properties in order to relate them to seismic observations such as amplitude and travel time. In this paper, the middle Frio clean sandstone reservoir rock density, bulk modulus, and velocity at Stratton field have been calculated. The empirical constants "free parameters" a, b, c were statistically estimated from the observed sonic velocity (Vp_{sonic}) and porosity (ϕ).The values of these best fit parameters are used to calculate the modulus of the dry porous rock frame (m_{dry}) which in turn is used to calculate the saturated plane-wave modulus (m_{sat}) and the velocity of the saturated porous rock frame (Vp_{sat}). The changes in the middle Frio rock parameters are predicted by the changes in the reflection coefficient (R_0) calculated at the top of the middle Frio reservoirs. The introduction of gas significantly decreases the rock velocity and density resulting in a negative reflection coefficient "amplitude dim spot effect".*

INTRODUCTION

Fields along the Vicksburg fault zone gas play FR-Play (Frio Reservoir gas Play) in south Texas such as Stratton field produce from multiple dispersed and concentrated sandstone pays in the Oligocene Frio Formation. In Stratton field (Fig. 1), a mature gas field, the Frio Formation is divided informally into lower, middle, and upper Frio (Fig. 2). Production comes mainly from the fluvial sandstone reservoirs of the middle Frio. Exploration efforts in the deeper middle Frio Formation gas reservoirs have typically been based on subsurface geology along with stratigraphic interpretation of seismic data (Kerr and Jirik 1990; Levey et al., 1993; and Hardage et al., 1994).

The middle Frio Formation, the object of this study, is the most important gas reservoir in the FR-Play in south Texas, Gulf Coast region. It consists of fluvial reservoirs represented by channel-fill and splay sandstones (reservoir deposits) bounded by non-reservoir floodplain mudstones and siltstones. For better understanding of exploitation and exploration of this reservoir it is important to determine its rock physics properties in order to relate them to seismic observations such as amplitude and travel time. To my knowledge, rock-physics properties of the sandstone reservoirs of the middle Frio Formation in Stratton field and in the FR-Play in south Texas have not been applied to exploration and exploitation.

Success of seismic data as a prospecting tool for fluvial deposits depends on using local information obtained from existing fields to carry out refined seismic modeling and interpretation. Seismic modeling of the middle Frio fluvial deposits at Stratton field in south Texas is twofold: building a rock physics predictive model, then using it to determine how rock property changes in the middle Frio would affect seismic response.

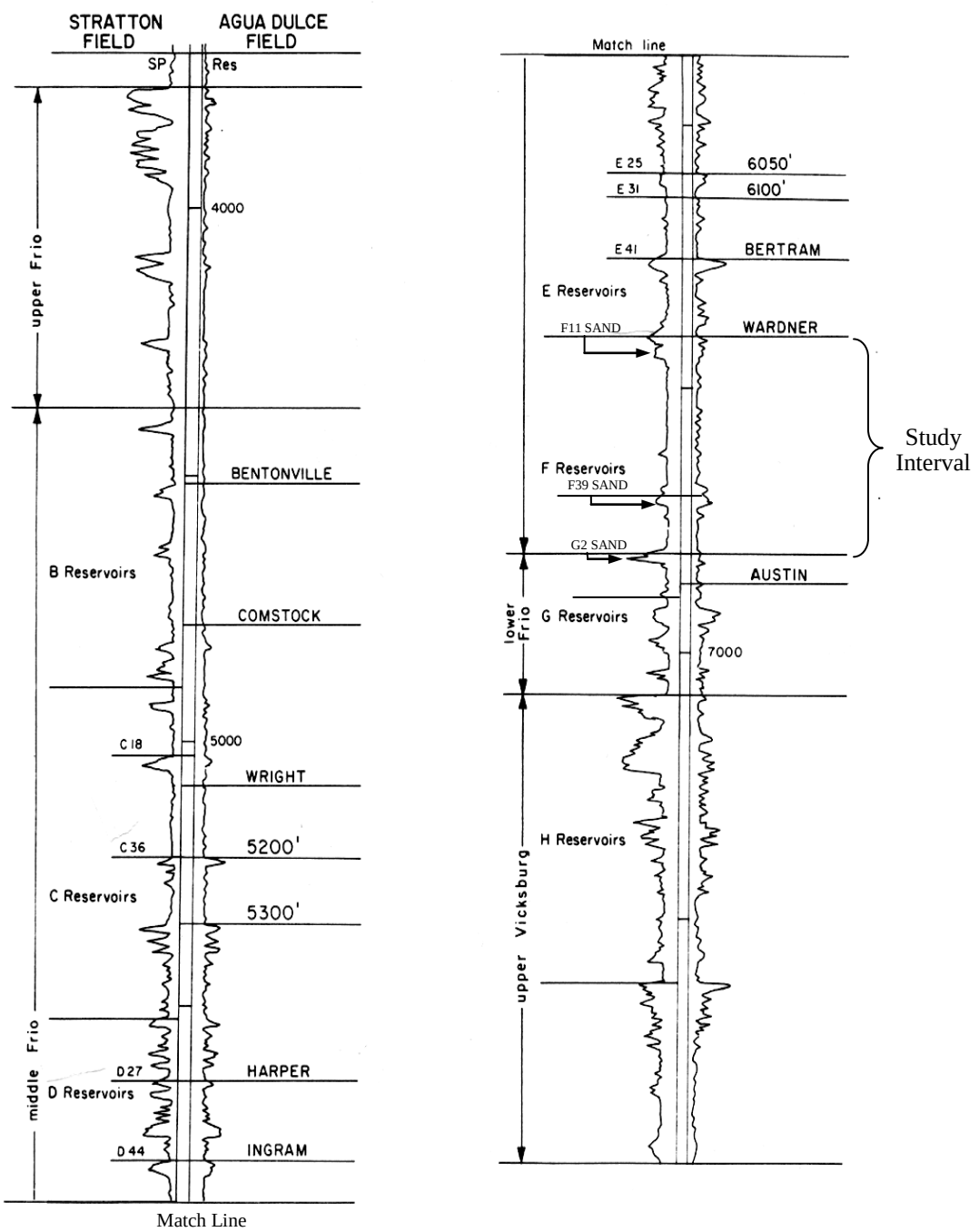

Figure 2: Type log from the Union Production Company Driscoll No. 7A well showing the Frio reservoir groups and nomenclature at Stratton (left) and Agua Dulce (right) fields (modified from Kerr, 1990).

Table 1. Average interval properties for middle Frio Formation (deeper F-series)

Parameter	Value	Units	Source of Information
Measured rock density (ρ)	2.65	g/cc	Core analysis by Bureau of Economic Geology UTA
Observed rock density (ρ)	2.195	g/cc	Density logs
Measured rock porosity (ϕ)	0.21	%	Core analysis by Bureau of Economic Geology UTA
Observed rock porosity (ϕ)	0.1-0.35	%	Neutron porosity logs
Observed *P*-wave velocity (Vp)	3717	m/s	Sonic logs
Reservoir pressure (P)	7.5	MPa	Levey et al., (1993)DOE Project Report #DE—FG21-88MC25031)
Reservoir temperature (T)	83	°C	Log header of well Wardner-184
Gas saturation (Sg)	0.55	%	Levey et al., (1993)DOE Project Report #DE—FG21-88MC25031)
Gas specific gravity (G)	0.65		Kosters et al., 1993 Atlas of Gas Fields, Texas and Levey et al., (1989)DOE Project Report #DE-FG21-88MC25031)
Formation water salinity (S)	17000	ppm	Levey et al., (1993) DOE Project Report #DE-FG21-88MC25031)
Frame stiffness constants (a, b,c)	(8.8, .16, 22.4)		Determined from both observed sonic velocity and neutron porosity
Quartz density (ρmin)	2.65	g/cc	Liner, C. L., 1999, Elements of 3-D Seismology. PennWell Scientific Publications. P-362.
Quartz bulk modulus (Kmin)	37900	MPa	Liner, C. L., 1999, Elements of 3-D Seismology. PennWell Scientific Publications. P- 362.
Quartz shear modulus (μmin)	44300	MPa	Liner, C. L., 1999, Elements of 3-D Seismology. PennWell Scientific Publications. P-362.

The middle Frio Formation is a major hydrocarbon producer in the Gulf Coast of the United States. Previous studies (Levey, et al.1993) indicated that untapped and incompletely drained reserves were encountered in the middle Frio reservoirs. Such results show good reason to search for and develop gas resources in the deeper middle Frio interval (F-series) in the study area. Therefore, detailed rock-physics properties of the sandstone reservoirs of the middle Frio Formation in Stratton field and in the FR-Play in south Texas is necessary to be calculated and be applied to exploration and exploitation for developing this mature reservoir.

Given the mature nature of the area, typical exploration targets are lower-potential stratigraphic traps in shallower productive intervals and higher-potential stratigraphic and fault-controlled compartments in the deeper middle Frio Formation.

Because of that, the Stratton field could be a good area for more development to find more bypassed compartments using an integrated interpretation and for time-lapse 3-D seismic (4-D) study. For 4-D seismic, it is important to evaluate the rock physics properties of the deeper interval of the middle Frio Formation in the study area.

Several theories have been developed that describe rock properties and their effects on seismic wave propagation in porous media (e.g. Gassmann, 1951; O'Connell and Budiansky, 1974; and Mavko, et al., 1998). In this work, reservoir rock density, bulk modulus, and velocity of the deeper middle Frio clean sandstone reservoirs at Stratton field area have been calculated. These properties depend on several important parameters and can be applied to bright-spot/dim-spot evaluation and log interpretation.

Reservoir pressure at seismic acquisition time is 1082 psi (7.5 MPa) (Levey et al., 1993) and temperature as measured in the Wardner 184 well is 181°F (83 °C). Average gas saturation of 0.55 was chosen as representative based on information from Wardner lease area in the Stratton field, (Levey et al., 1993). Table 1 shows the sources of these and other parameters used to calculate reservoir rock properties of the middle Frio Formation at Stratton field. The relationships used in these calculations are drawn primarily from Batzle and Wang (1992) and Liner (1999).

ROCK PROPERTY EVALUATION

Better understanding of the rock properties of the middle Frio Formation can be achieved by estimating reservoir rock physics properties such as density and velocity. Figure 3 is a flow chart showing the procedure followed in rock property evaluation.

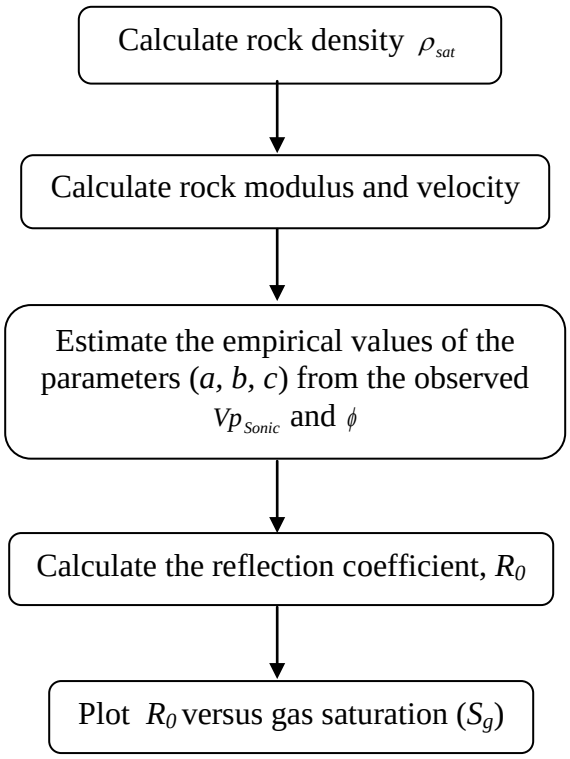

Figure 3: Flowchart of the procedure followed in rock property evaluation.

Rock density

The density (ρ_{sat}) of the porous, fluid saturated (gas and brine) middle Frio sandstone reservoir rocks can be calculated from the following equation

$$\rho_{sat} = \rho_{\min}(1-\phi) + \phi\rho_f \qquad (1)$$

where $\rho_{\min}$ is the density of quartz (g/cc), ρ_f is the fluid mixture density (g/cc), and ϕ is the fractional porosity (core-derived porosity of 21%). This equation yields a density of 2.170 g/cc for the deeper middle Frio sandstones assuming gas saturation and water saturation as 55% and 45%, respectively. In comparison, the observed bulk density of the middle Frio sandstone reservoirs estimated from the density logs of Wardner 224 and Wardner 226 wells of Stratton field is 2.195 g/cc.

Rock modulus and velocity

The next step is to calculate rock modulus and velocity. For velocity calculations, three kinds of moduli are involved. These are bulk modulus (κ), plane-wave modulus (*m*) and shear modulus (μ). The relation between bulk moduli of the mineral component, dry rock frame, and saturated rock frame is called the Gassmann theory (Liner, 1999). Gassmann's relations use the difference between the dry rock bulk modulus and mineral modulus to ascertain the compressibility of the pore space. Rock shear modulus is assumed to be unaffected by fluids.

The mineral *P*-wave modulus m_{min} is given by

$$m_{\min} = k_{\min} + \frac{4}{3}\mu_{\min} \tag{2}$$

where $k_{\min}$ and $\mu_{\min}$ are the sandstone (quartz) bulk and shear moduli (MPa), respectively (Table 1).

The modulus of the dry porous rock frame (m_{dry}) characterizes the stiffness of the rock. This modulus can be estimated from the following nonlinear relationship

$$m_{dry} = m_{\min}/(1 + a\phi + b\phi^2 + c\phi^3) \tag{3}$$

where *a, b and c are* empirical constants of the rock. A smaller value of "*a"* means the rock is soft or poorly consolidated, and a larger value means it is hard and well cemented. One-way to estimate the value of the frame stiffness constant "*a*" is from laboratory measurements on dry cores. In the absence of *P*-wave velocities on cores the empirical constants "free parameters" a, b, c can be statistically estimated from the observed sonic velocity (Vp_{sonic}) and porosity (ϕ). Sonic values can be converted to rock *P*-wave speed in ft/s using the following equation

$$V_p = \frac{1{,}000{,}000}{Sonic\,time(\mu s/\,ft)} \tag{4}$$

The observed sonic velocity (Vp_{sonic}) plotted against the porosity (ϕ) of the selected deeper middle Frio clean sand intervals (Fig. 4). The values of the free parameters a, b, and c are statistically estimated as a = 8.84, b = 0.16, and c = 22.4. The values of these best fit parameters used to calculate the modulus of the dry porous rock frame (m_{dry}) which in turn used to calculate the saturated plane-wave modulus (m_{sat}) and the velocity of the saturated porous rock frame (Vp_{sat}). In order to evaluate how good the fit is, the residual values are plotted against the fitted V*p* values (Fig. 5). Fit residuals are the differences between the observed responses and the predicted responses. The predicted responses are the fitted V*p* values obtained by evaluating the best fit function at the observed values of the independent ϕ variable. The plot (Fig. 5) indicates high correlation which implies good fit between the observed sonic velocity (Vp_{sonic}) and porosity (ϕ).

The velocity of the saturated porous rock frame (Vp_{sat}) is given by the following relationship

$$V_{p_{sat}} = \sqrt{1000 m_{sat}/\rho_{sat}} \tag{5}$$

where m_{sat} is the saturated rock plane-wave modulus in MPa, which is determined from the following equation

$$m_{sat} = \frac{m_{\min}\left(\frac{m_{dry}}{m_{\min} - m_{dry}} + \frac{K_f}{\phi(m_{\min} - K_f)}\right)}{1 + \left(\frac{m_{dry}}{m_{\min} - m_{dry}} + \frac{K_f}{\phi(m_{\min} - K_f)}\right)} \tag{6}$$

where k_f is the fluid mixture modulus (MPa).

REFLECTION COEFFICIENT

Armed with the rock model for the deeper middle Frio sandstone reservoirs, it is important to predict how changes in reservoir parameters will influence seismic observables such as amplitude. This is done by calculating the reflection coefficient (R_0) at the top of the middle Frio reservoirs. The normal incidence reflection coefficient for an interface is a function of *P*-wave velocity and density on either side of the interface.

To calculate the reflection coefficient, the *P*-wave velocity and density of the cap rock (middle Frio floodplain mudstones) should be known, and then the reflection coefficient can be calculated from

$$R_0 = \frac{\rho_2 V_2 - \rho_1 V_1}{\rho_2 V_2 + \rho_1 V_1} \tag{7}$$

where ρ_1, V_1 are the density and velocity of the cap rock, and $\rho_2 = \rho_{sat}$, $V_2 = V_{sat}$ are the calculated density and velocity of the reservoir rock.

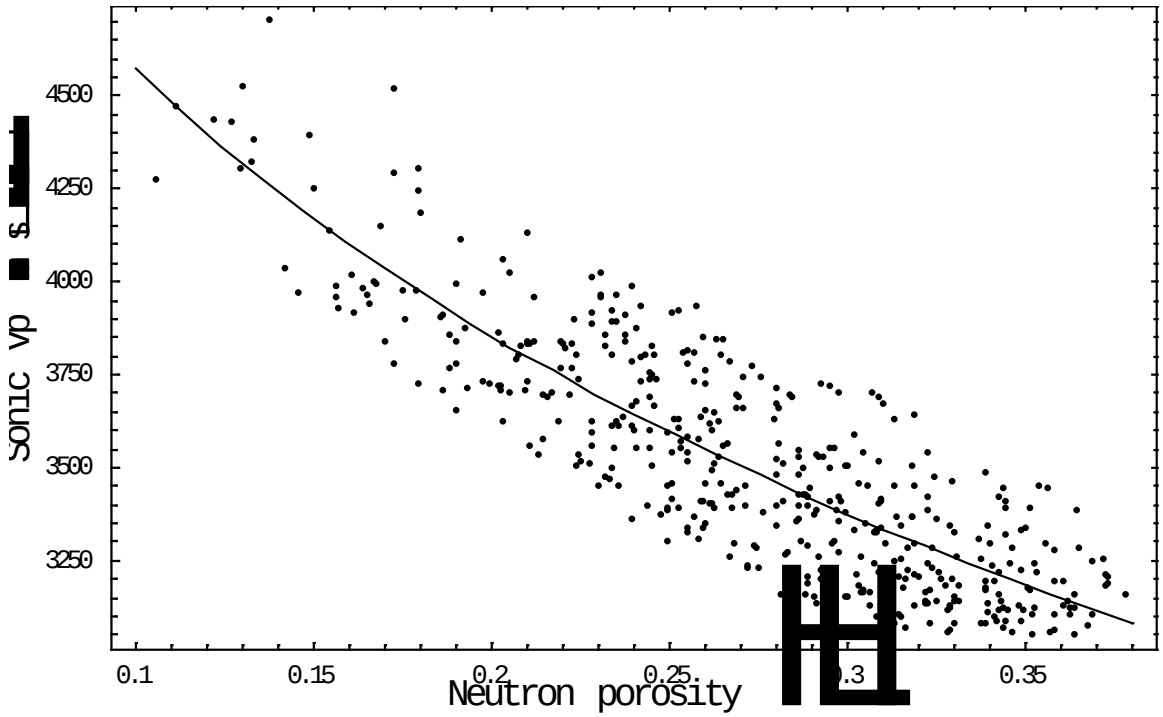

Figure 4: Observed velocity-porosity plot used to estimate the free parameters (*a, b and c*) of the deeper middle Frio clean sandstone reservoirs.

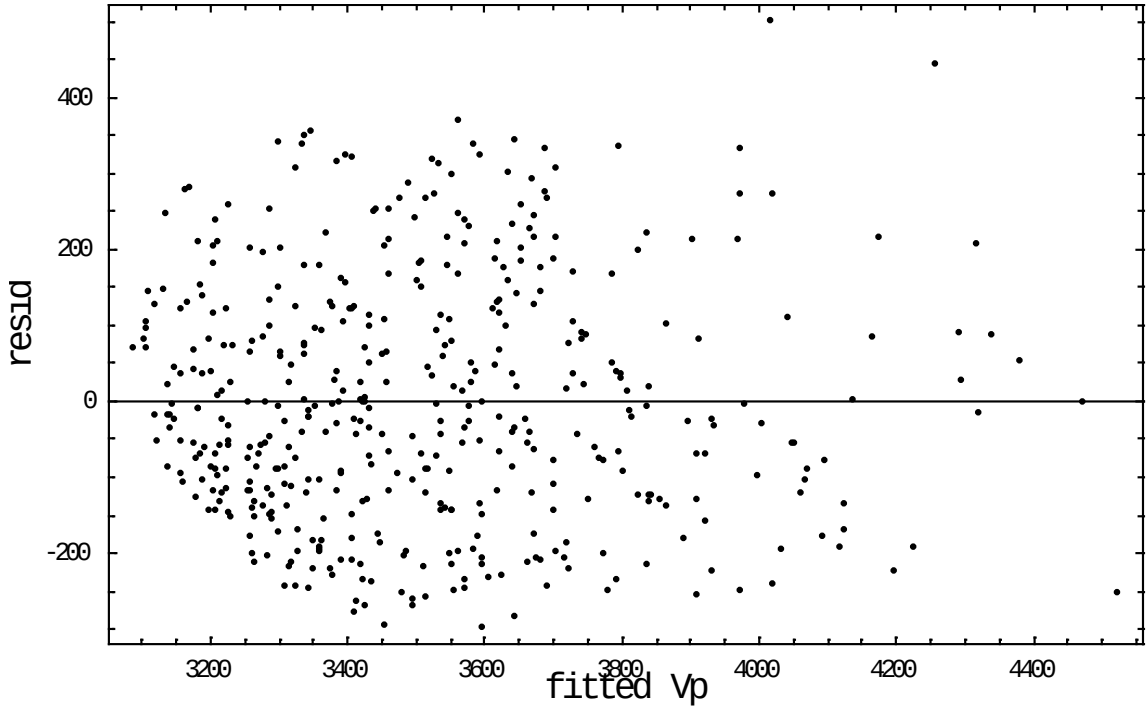

Figure 5: Plot showing a good fit between the residuals and fitted V*p*.

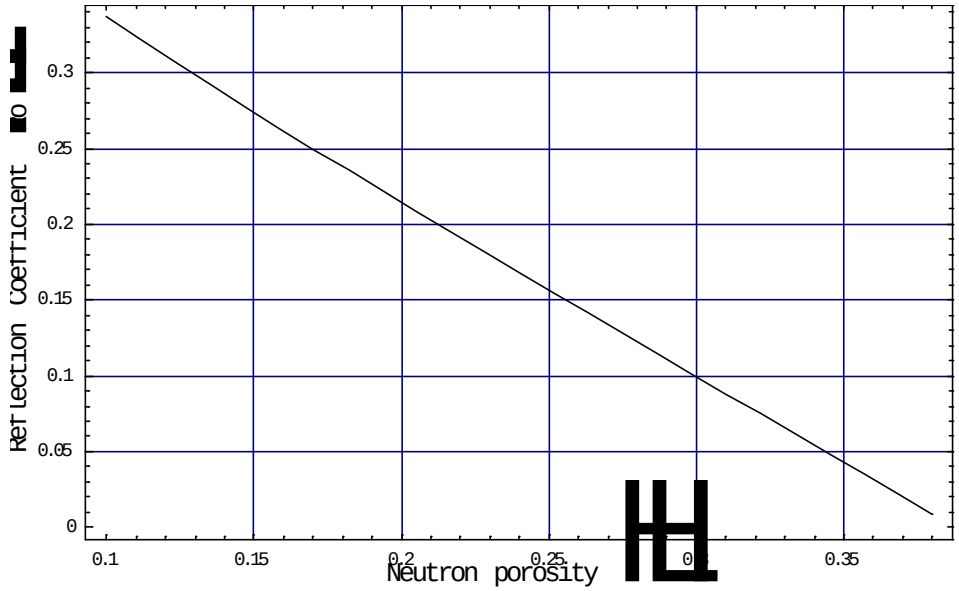

Figure 6: Plot of reflection coefficient *(R_0)* as a function of porosity. Changes in porosity result in significant change in the R_0. For example, increasing porosity from 15% to 25% reduces reflection coefficient from 0.28 to 0.16, a 43% drop in amplitude.

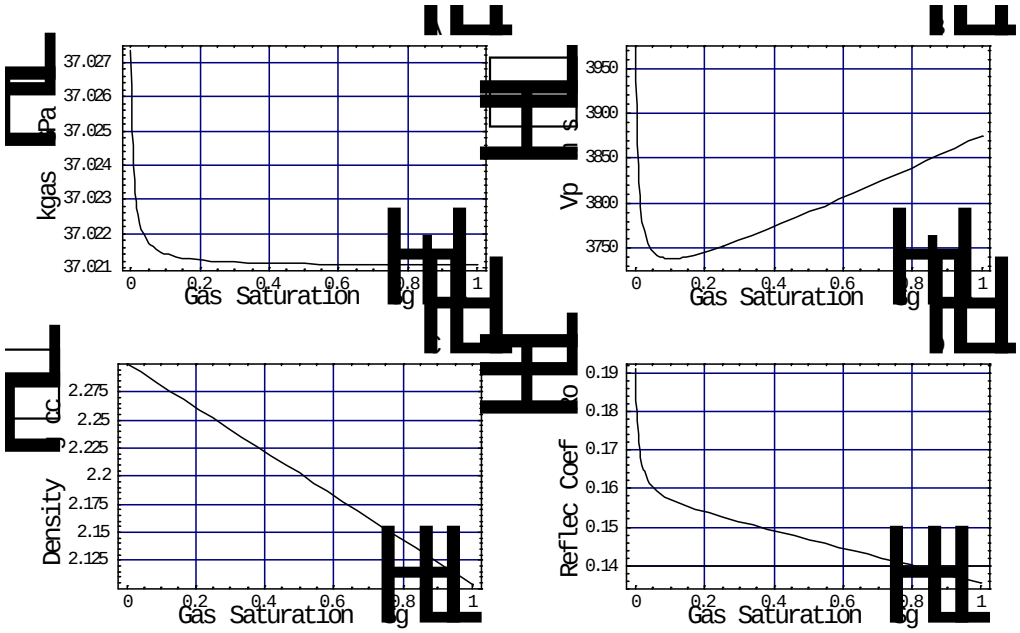

Figure 7: Effect of gas saturation on the reflection coefficient (R_0) for the given set of rock parameters. Fractional porosity is fixed at 21%. (A) Increasing gas saturation causes an abrupt decrease in the saturated-rock bulk modulus. (B) Increasing gas saturation causes drastic reduction in rock velocity until 0.16 Sg and then starts to increase again. (C) Increasing gas saturation also causes a significant decrease in density. (D) The combined effect of decreasing rock bulk modulus, velocity, and density causes a decrease in R_0, i.e., amplitude dim spot effect.

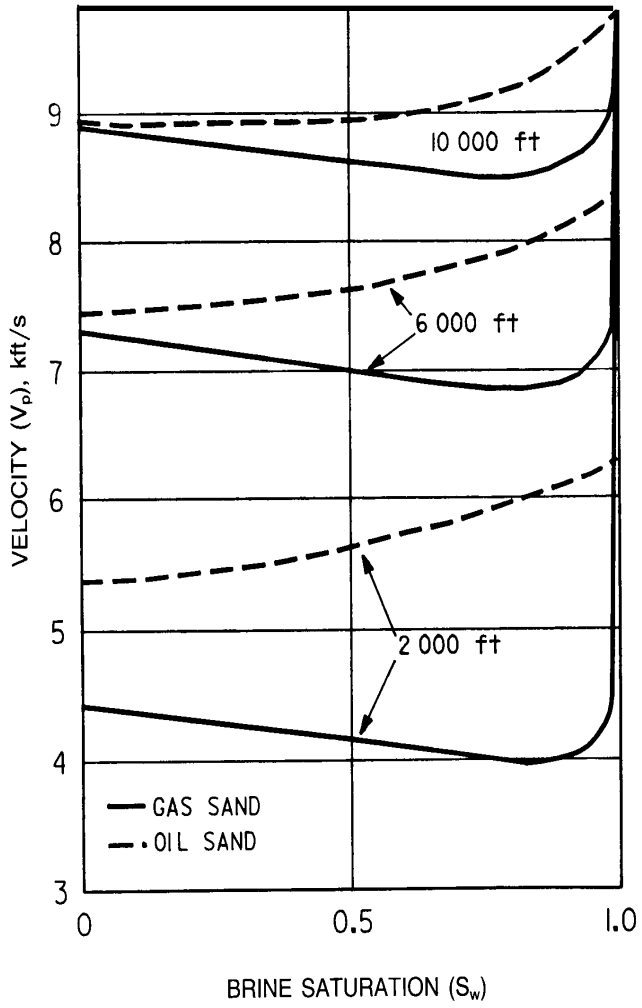

Figure 8: *P*-wave velocity as a function of water saturation (S_w) for gas and oil sands at different depths (From Domenico, 1974). Notice that the response of the V*p* due to the gas as a second pore fluid at 6000 ft depth is similar to that of the deeper middle Frio gas sands (Fig. 7.B).

The above relation is also a measure of R_0 at fluid interfaces within the rock. Usually R_0 is maximum at liquid-gas interfaces or at interfaces between liquids and liquid gas mixtures of high gas content. Figure 6 is a plot showing the effect of porosity changes on the reflection coefficient for the middle Frio sandstone reservoirs.

FLUID SUBSTITUTION

Calibration of the basic seismic response to real reservoir rock parameters is critical to the interpretation of the variations observed in seismic data. One of the most important problems in rock physics analysis of logs, cores, and seismic data is the prediction of seismic velocities in rocks saturated with one fluid from rocks saturated with a second fluid—or is the prediction of saturated rock velocities from dry rock velocities, and vice versa (Mavko et al., 1998).

Changes in a rock can be predicted by changes in the reflection coefficient. The introduction of gas significantly decreases the rock velocity and density resulting in a negative reflection coefficient (Fig. 7). Mavko et al. (1998) noted that by introducing fluids into the dry rock, the dry rock velocity drops by a certain amount.

The middle Frio gas-sand velocity abruptly decreases as the gas saturation increases from zero (100 % brine) to a gas saturation of approximately 0.16 (84 % brine) and then increases to the velocity of fully gas-saturated sand reservoir (Fig.7-B). This velocity behavior is similar to that of the gas-sand as a function of water saturation obtained for the Tertiary shale and sand sequences of the Gulf Coast basin (Fig. 8) (after Domenico, 1974).

CONCLUSION

Reservoir rock properties such as density, bulk modulus and velocity are important to study. They aid in petroleum exploitation and exploration by establishing a correlation between the seismic attributes and rock properties. In this work, the rock physics properties of the F-series reservoir rocks of the middle Frio Formation of Stratton field were evaluated and related to the normal incidence reflection coefficient. Also the effect of introducing fluids such as gas to water wet sandstone on the rock *P*-wave velocity, density, and reflection coefficient has been estimated.

ACKNOWLEDGEMENTS

The author is grateful to the Geosciences Department of the University of Tulsa, Oklahoma, USA, especially Dr. Christopher Liner and Dr. Dennis Kerr, for providing the necessary data and software to accomplish this work and for their useful comments.

REFERENCES

Batzle, M. and Wang, Z., 1992, Seismic properties of pore fluids, Geophysics, Vol. 57, no. 11, pp. 1396-1408.

Domenico, S. N., 1974, Effect of water saturation on seismic reflectivity of sand reservoirs encased in shale: Geophysics, Soc. of Expl. Geophys., 39, 759-769.

Gassmann, F., 1951, Elastic waves through a packing of spheres: GEOPHYSICS, Soc. of Expl. Geophys., 16**,** 673-685.

Hardage, B.A.; Levey, R.A.; Pendelton, V.; Simmons, J.; and Edson, R., 1994, A 3-D seismic case history evaluating fluvially deposited thin-bed reservoirs in a gas-producing property. Geophysics. Vol. 59, No. 11; P.1650-1665.

Kerr, D.R., and Jirik, L.A., 1990, Fluvial architecture and reservoir compartmentalization of the Oligocene Middle Frio Formation, South Texas: Gulf Coast Association of Geological Societies Transactions, v. 40, p. 373-380.

Kosters, E.C., Bebout, D.G., Seni, S. J., Garrett. M., Jr., Brown, L.F. Jr., Hamlin, H.S., Dutton, S.P., Ruppel, S.C., Finely, R.J., and Tyler, Noel, 1989, Atlas of major Texas Gas Reservoirs: The University of Texas at Austin, Bureau of Economic Geology Special Publication, pp.1-161.

Levey, R.A.; Hardage, B.A.; Langfordf, R.P.; Scott, A.R.; Finely, R.J.; Fisher, W.L.; Sippel, M.A.; Collins, R.E.; Vidal, J.M.; Howard, W.E.; Ballard, J.R.; Grigsby, J.D.; Kerr, D.R., **1993**, Secondary natural gas recovery: targeted technology applications for infield reserve growth in fluvial reservoirs, Stratton Field, South Texas. Topical report for the Gas Research Institute contract No. 5088-212-1718 and US Department of Energy contract No. DE-FG21-88MC25031, 244p.

Liner, C.L., 1999, Elements of 3-D Seismology. PennWell Scientific Publications. 438p.

Mavko, G., Mukerji, T, and Dvorkin, J., 1998, The rock physics handbook, tools for seismic analysis in porous media. Cambridge University press, 180 p.

O'Connell, R.J. and Budiansky, B., 1974, Seismic velocities in dry and saturated cracked solids: Journal of Geophysical Research, v. 79, no. 35, 5412-5426.

Egyptian Geophysical Society
EGS Journal, vol. 3, No. 1, 27-34 (2005)

RECENT 3-D LOCAL MIGRATION OF SEISMIC EVENTS AND STRESS DISTRIBUTION IN THE NORTHERN RED SEA, SAUDI ARABIA

Nassir S. Al-Arifi

Department of Geology, King Saud University, P. O. Box 2455, Riyadh 11451, Saudi Arabia
E-mail: nalarifi@ksu.edu.sa

الارتحال المحلى ثلاثى الأبعاد للأحداث الزلزالية وتوزيع الاجهادات فى شمال البحر الأحمر / المملكة العربية السعودية

الخلاصة: اعتبر خليج العقبة خلال الخمس عشرة سنة الأخيرة من المناطق النشطة زلزالياً فى منطقة الشرق الأوسط، فصدع النقل ذو الانزلاق المضربى والذى يضم خليج العقبة – البحر الميت بطول ١١٠٠كم والذى يربط بين منطقة طوروس – زجروس (جنوب تركيا – غرب إيران) بخسف البحر الأحمر يمكن إرجاعه إلى الظواهر ذات النشاط التكتونى العظيم.

أعد العريفى (١٩٦٦) والشعبى (١٩٩٨) قائمة من ١٤١٥ زلزالاً (≤ ٢,٨ درجة) تغطى فترة زمنية من عام ١٩٨٥ إلى عام ١٩٩٥ وتعتمد هذه القائمة السيزمية للمملكة العربية السعودية، حيث تغطى هذه البيانات مساحة تقع بين خطى عرض ٢٨ ° و ٣٠° شمالاً وبين خطى طول ٣٠ ° و ٣٦° شرقاً وقد استخدمت البيانات لدراسة الارتحال المكانى للتوابع الزلزالية خلال عامى ١٩٩٣ و ١٩٩٥، حيث تم حساب توزيع الاجهادات منها. وقد وجد أن الاتجاه المتوسط للاجهادات الدنيا هو ٢٢٢° بينما يأخذ الاتجاه المتوسط للاجهادات العظمى ١٣٧° .

وقد وجدت هذه القيم فى توافق تام مع الاستنتاجات الجيولوجية الأساسية لاتجاهات الاجهادات والتى تأخذ إتجاه شمال – شمال غرب للقيم العظمى الشبه الأفقية، كما وجد أن التوابع الزلزالية قد ارتحلت شمالاً لمسافة ٦٠كم لتتابع عام ١٩٩٣ وحوالى ٧٠كم لتتابع عام ١٩٩٥، كما أن التوابع قد ارتحلت لبؤر ضحلة العمق حيث كان عمق الزلزال الرئيسى لعام ١٩٩٣ هو ١٥كم وعمق التابع القوى الأخير (٥,٢ درجة) له ٢ كم. وقد أحدث الزلزال الرئيسى فى عام ١٩٩٣ إعادة إنتشار للاجهادات على أجزاء الصدوع المتوازية، كما أن حدوث التابع الضخم لزلزال عام ١٩٩٣ قد أطلق أجزاء الصدوع لتكون منطقة النواة التى نشأ عليها الزلزال الرئيسى عام ١٩٩٥.

ABSTRACT: *During the last 15 years, the Gulf of Aqaba has been considered one of the most seismically active regions in the Middle East. The 1100 km long strike-slip Gulf of Aqaba-Dead Sea transform fault is a major active tectonic feature linking the Taurus-Zagros area of southern Turkey- western Iran with the Red Sea rift. A catalogue of 1415 earthquakes (MD ≥ 2.8) covering a time span from 1985 to 1995 were compiled by Al-Arifi (1996), Al-Shaabi (1998). It is mainly based on data from King Saud University, Seismic Studies Centre (SSC), Kingdom of Saudi Arabia. It covers an area extent from 28°N to 30°N and from 30°E to 36°E. The catalogue has been used to study local migration of aftershocks during the 1993 and the 1995 sequences. It is also used to calculate the stress distributions of (σ1 and σ3). The mean direction of the minimum stress σ3 was found 222°. While the mean direction of the maximum stress σ1 was 137°. These values are in good agreement with the geologically inferred principal stress directions for the region, which indicate north-northwest-trending, maximum compressive stress (σ1) and northeast-trending, near-horizontal minimum compressive stress (σ3). The aftershocks migrate northwards about 60 km for the 1993 sequence and about 70 km for the 1995 sequence. The aftershocks migrate also to shallow focal depths, where focal depth of the 1993 main-shock is 15 km, to 2 km for the last strong aftershock (MD=5.2), which occurred in the late stage of the sequence. The 1993 main-shock caused re-distribution of stresses to the parallel faults segments where the 1993 largest aftershock occurred that triggered these fault segments to be area of stress nucleation and generated the 1995 main-shock.*

INTRODUCTION

The 1100 km long strike-slip Gulf of Aqaba-Dead Sea transform fault is a major active tectonic feature linking the Taurus-Zagros area of southern Turkey-western Iran with the Red Sea rift. Its left-lateral strike-slip motion is suggested to be a result of the relative oblique left hand movement between Arabia and Africa plates to open up the Red Sea (Quennell 1958, 1959; Freund et al., 1970).

In the southern Dead Sea transform fault which represents the Gulf of Aqaba, indicated that, the movement started in the late Miocene which is associated with a strike-slip stress pattern (40° direction of extension associated with a 130° compression). This movement produced the left lateral motion between the Arabian plate and Sinai Peninsula and since the end of the Miocene the faulting is the result of an E-W extension, which indicates a rotation of the regional stress pattern in the vicinity of the transform fault. Using the focal mechanism solution for 53 recent earthquakes in the Gulf of Aqaba, Al-Arifi (1996) found that, the main direction of the maximum compressive stress (σl) in 137° and the main direction of the minimum stress (σ3) in 222°.

The structure of the Gulf is dominated by en-echelon normal faults, which delimit three elongated basins (Ben-Avraham et al., 1979, Reiss and Hottinger 1984). The northern basin has a simple bathymetry and structure, dominated by the flat- bottomed Eilat deep

(<900 m). The central basin consists of two deeps: Aragonese deep (<1850m), and Arnona deep (<1550m). The southern basin includes the Dakar (<1400m) and Tiran (<l300m) deeps (Figure 1).

In this paper, two main objectives are considered. The first objective is to outline the local migration of aftershocks in vertical and horizontal directions for the most recent sequences (i.e. the 1993 and the 1995 sequences). The second objective is to presents some observations of stress migration that caused large earthquake in the Gulf.

RECENT SEISMICITY

The Gulf of Aqaba has been considered one of the most seismically active regions of the Middle East during the last 15 years. A catalogue of 1415 earthquakes (duration magnitude $MD \geq 2.8$) for 1985-1995 has been compiled by Al-Arifi 1996 and A1-Shaabi 1998. It is based mainly on data from Seismic Studies Centre (SSC), King Saud University, Saudi Arabia. It covers an area from 28°- 30° N and 30°-36° E. Historical seismicity (1068-1964) shows that the region suffered at least 18 moderate to large earthquakes. Instrumental seismicity (1965-1984) includes 284 events, 244 of which were the 1983 sequence centered on the Eilat deep in the northern Gulf. Recent seismicity (1985-1995) shows that, the Gulf of Aqaba seismicity has been episodic (Figure 2). In July 1993 an earthquake sequence began with foreshocks, followed by a mainshock (MD=6.0) on August 3, 1993, and then 403 aftershocks ($MD \geq 2.8$) in four months with magnitude of 5.6 for largest aftershock (Figure 3a). On November 22nd 1995, the region experienced a widely-felt earthquake located at 28.81° N, 34.75° E with a focal depth of 12 km. The mainshock (MD=6.2) was followed by 733 aftershocks ($MD \geq 2.8$) in 40 days with magnitude of 5.3 for largest aftershock (Figure 3b).

The 1983 sequence concentrates in the north part of the Gulf of Aqaba (28.8°- 29.4° N and 34.3- 35.l° E). Most of this sequence is offshore and coincides with the Eilat deep. Although, the determination of depth was difficult because of lack of stations. El-Isa et al., (1984) observed the surface waves clearly in the records of the Jordan University seismic station which suggest very shallow depth for the 1983 sequence. Their observation is supported by the recent SSC recorded earthquakes which are located in the same area that suffered from the 1983 sequence. These earthquakes are located at a shallow depth not exceeding 10 km (A1-Shaabi 1998). The 1993 sequence was concentrated in the Dakar and Tiran deeps in the southern part of the Gulf with focal depths did not exceed 26 km. The 1995 sequence distributed in two clusters, the northern cluster of which was again concentrated in the Eilat deep, whereas the southern cluster was in the Aragonese and Arnona deeps in the central Gulf. The depth of the 1995 sequence is generally less than the 1993 sequence. This may be because of the location of aftershock zone, where the 1993 aftershock zone concentrated in the southern part of the Gulf whereas the 1995 aftershock zone spread along the Gulf and the density of aftershock was greater in the northern part than the southern part. This may indicate that the earthquakes which occur in the northern part are shallower than the ones in the southern part of the Gulf and relate to the brittle-ductile transition zone (Al- Shaabi 1998). This observation is supported by the 1995 aftershocks where the events in the northern cluster are shallower than the ones in the southern cluster. In addition, the surface waves appear clearly when the earthquakes are located in the north of the Gulf of Aqaba (A1-Shaabi 1998). However, they disappear from the records when they are located in the south.

LOCAL MIGRATION OF AFTERSHOCKS

In order to study the local migration of aftershocks both vertically with depth and horizontally along a NE-SW direction it is required to delineate the tectonic setting of the area of interest. That corresponds to the general state of extensional tectonic stress in the Gulf of Aqaba and the Dead Sea Transform, according to small scale structures study (Reches, 1987), and focal mechanisms study (Al-Arifi, 1996). We shall use the term ‘local migration’ to denote the movement of a strong aftershock tends to move horizontally during the sequence. We shall also use the term ‘jumping’ to denote the movement a strong aftershock in the vertical direction. The term strong aftershock in this paper means the aftershocks which are felt at least in three towns of the study area. Because all strong aftershocks occurred at a shallow depth not exceeding 20 km all aftershocks with magnitude of 4.9 and over were felt at least in three towns.

The 1993 mainshock occurred at the extreme south end of aftershock zone at 28.45°N and 34.87°E (Figure 3a). The aftershocks moved in a general northward direction.

Figure 4a shows the local migration of the strong aftershocks of the 1993 sequence. On the same day which the mainshock occurred, the activity concentrated in the north between 28.70-28.8S° N and 34.75-34.9° E, where two strong aftershocks with magnitude of 5.6 and 4.9 occurred. 80 days after the mainshock the activity moved northwards again where another strong aftershock occurred at 29.0° N and 34.83° E. On the 3/11/1993 the activity leaped to the south-west (still north of the mainshock) with another strong shock that occurred at 28.62° N and 346, the activity moved northwards where the last strong aftershock occurred on 4/12/1993 at 28.86° N and 34.41° E.

In addition, figure 4b shows that the focal depth of the 1993 started with more than 10 km for foreshocks with no foreshocks having a depth less than 10 km. The mainshock had the depth of 15 km and then the depth reduced with time from 11-12 km for the first two strong aftershocks until the last strong aftershock was at

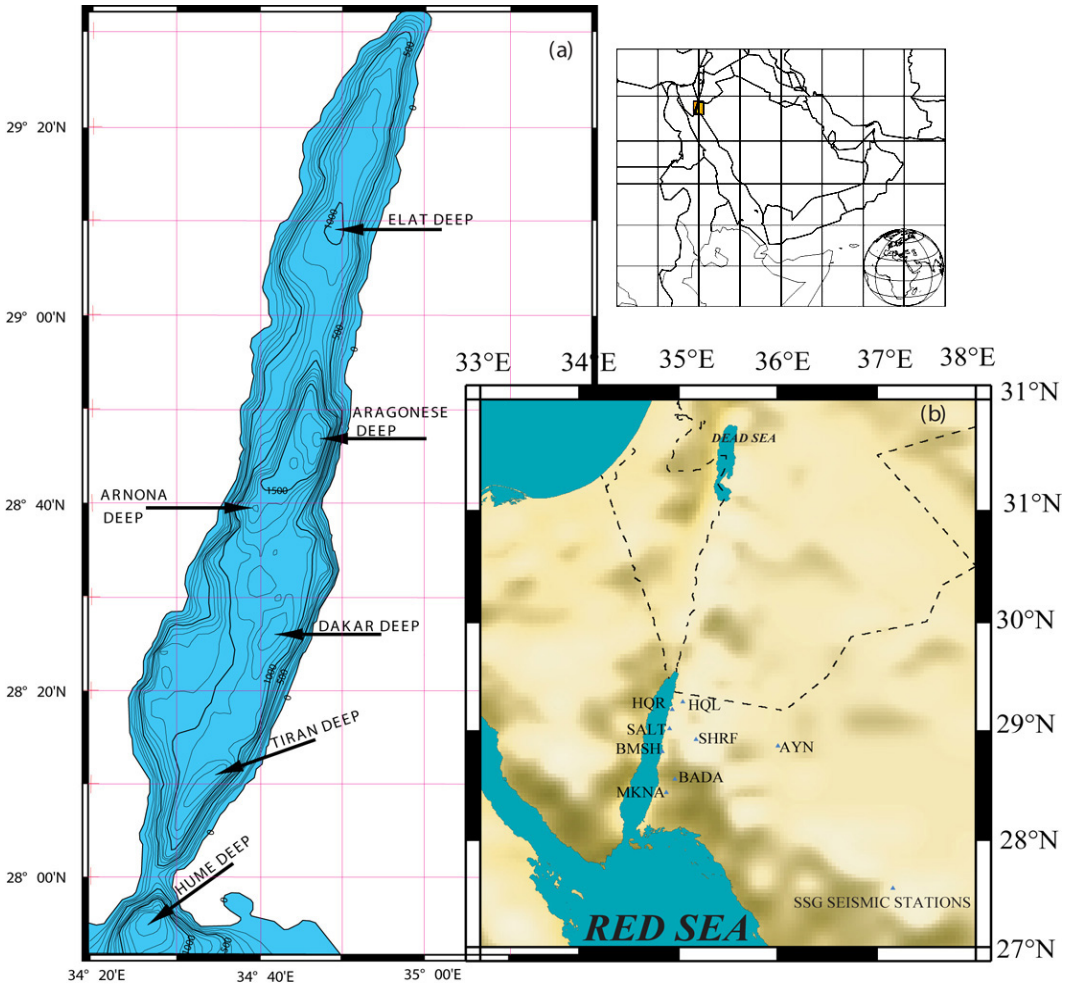

Figure (1): Index map showing the location of the study area in addition to (a) Bathymetric chart of the Gulf of Aqaba (Bathymetric map after Hall and Ben-Avraham, 1978), (b) location map of the SSG deismic stations.

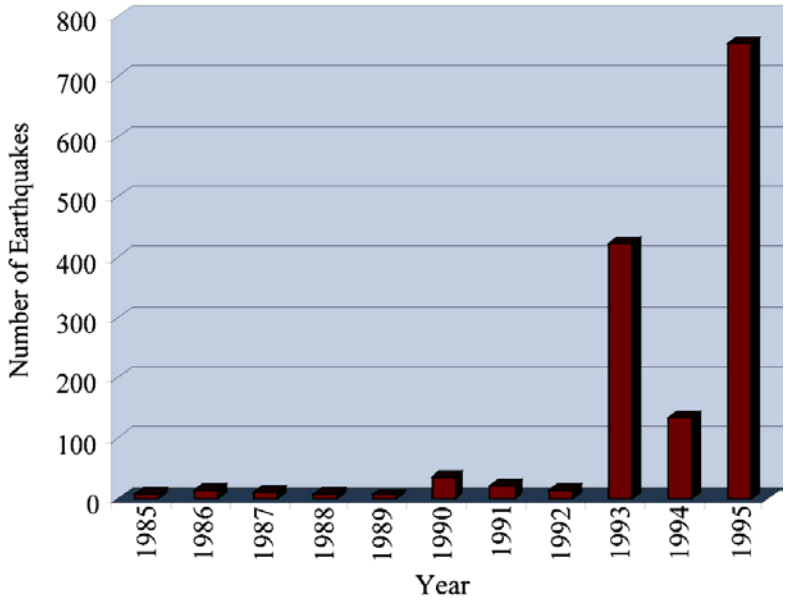

Figure (2): A histogram showing the frequency of occurrence (number of events/day) in the Gulf of Aqaba from 1985 to 1995.

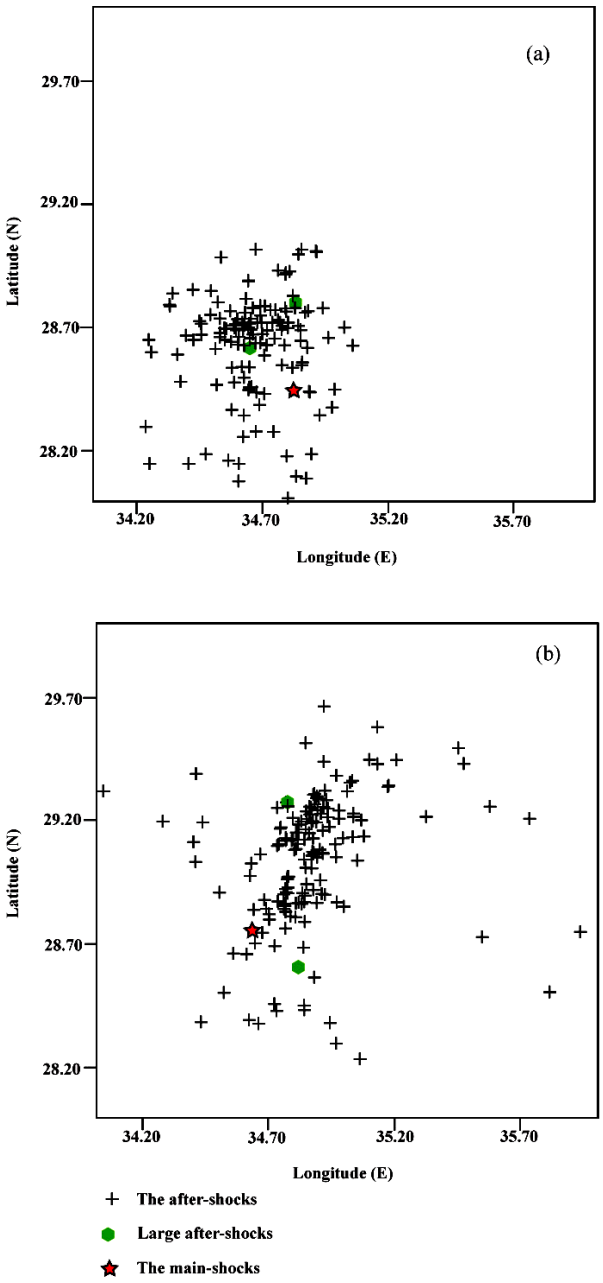

Figure (3): Epicentral distributions of earthquakes (MD>3.5) for two sequences. Where A is the 1993 sequence and B is the 1995 sequence. Small and large arrows indicate the direction of the minimum and maximum compressive stresses respectively, according to small scale structures study (Reches 1987), and focal mechanism study (Al-Arifi 1996).

a depth of 2 km. The 1995 sequence is similar, the focal depths of the aftershocks reduces with time. This 'jumping' feature may be explained by the fact that the earthquakes migrate northwards into area where all seismicity is shallower than in the south of the Gulf. As regards the local migration of the 1995 sequence, it was difficult to determine a specific direction for strong aftershock, but the aftershocks moved in general northwards.

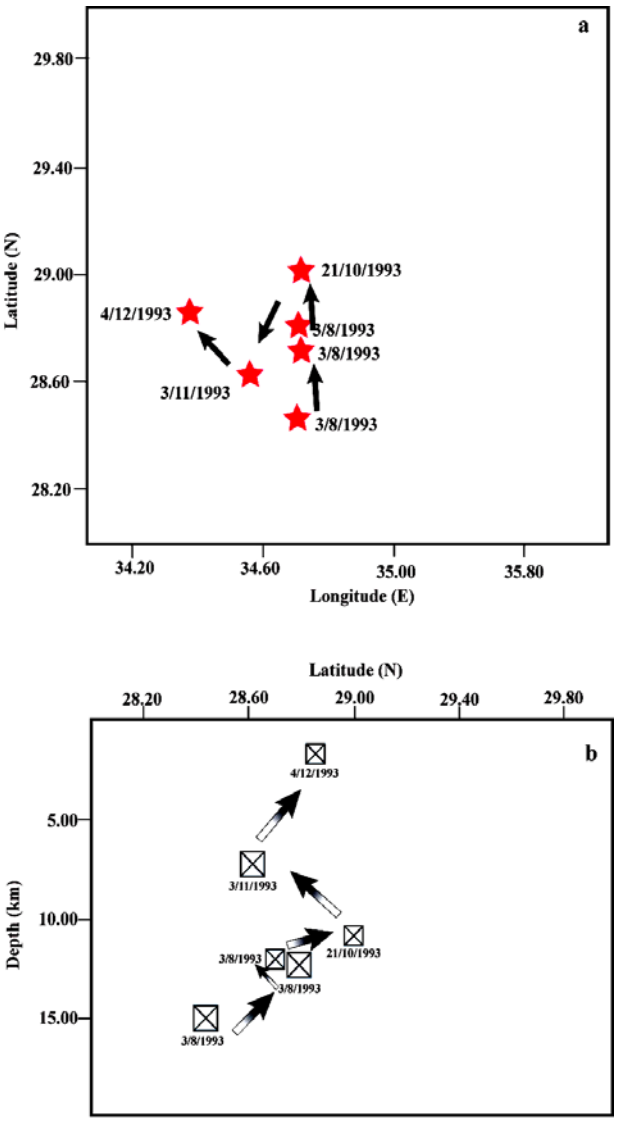

Figure (4): (a) Shows the local migration of strong aftershocks of the 1993 sequence in the Gulf of Aqaba. (b) Shows Profiles for jumping of strong aftershocks of the 1993 Gulf of Aqaba sequence. The arrows indicate the direction of the local migration and jumping.

SYSTEMATIC MIGRATION OF MODERATE EARTHQUAKES

The focal mechanism solution for the main-shocks and the largest aftershocks for both sequences of the 1993 and 1995 (Figure 5) include the following:

1. The 1993 mainshock indicates normal and strike-slip fault dipping 34° to the northwest and striking N 21° E.
2. The 1993 largest aftershock which occurred 3 hours and 50 minutes after the main shock indicates left-lateral strike-slip fault dipping 64° to the north and striking E 4° S.

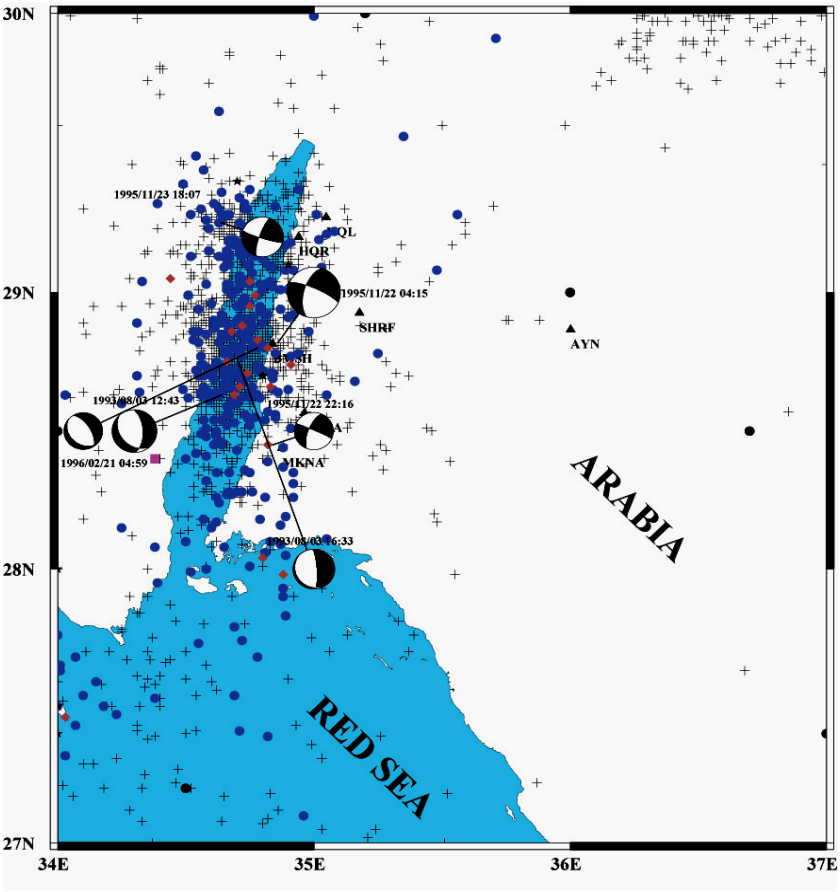

Figure (5): Shows the focal mechanism solution for the main-shocks and the largest aftershocks for both sequence of the 1993 and 1995.

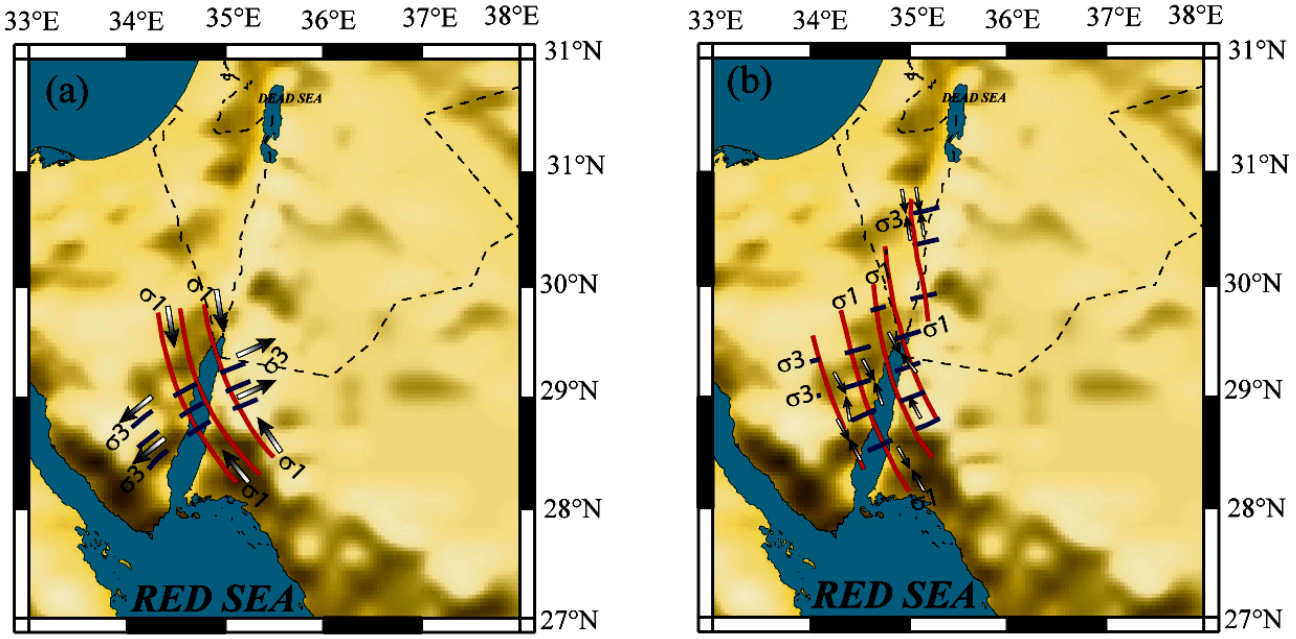

Figure (6): The mean direction of the minimum stress σ3and the mean direction of the maximum stress σ1: (a) by Al-Amri (1990) and (b) by Reches (1987).

3. The 1995 mainshock indicates left-lateral strike-slip fault dipping 43° to the north and striking N 09° E.
4. The 1995 largest aftershock that occurred after 35 hours from the mainshock indicates normal and strike-slip fault dipping 31° to the northwest and striking 198°.

Observations of these focal mechanism solutions and locations of the main-shocks and the largest aftershocks of both Gulf of Aqaba sequences (i.e the 1993 and the 1995 sequence) indicate the following:

1. For both sequences, the seismic sources of the main-shocks and its largest aftershocks where completely different (Figure 5).
2. The seismic source of the 1993 largest aftershock and the 1995 mainshock where located on the same fault zone (Figure 5).
3. There is a systematic migration of seismic sources of the earthquakes from south to north (Figures 4 and 5). This systematic northward migration is influenced by the main direction of the maximum tectonic stress in the Gulf of Aqaba which takes direction of 137° as found by Al-Arifi (1996).

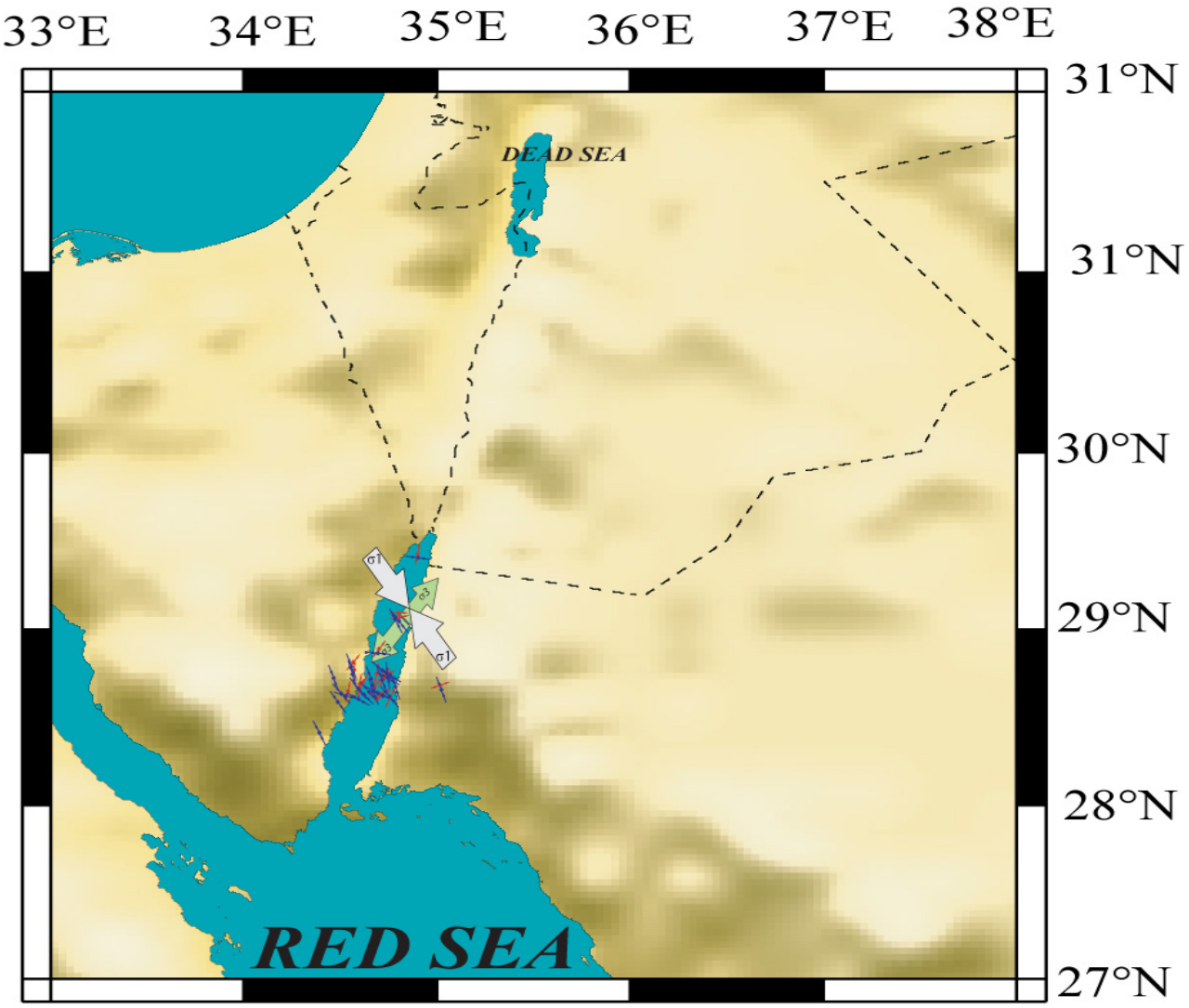

Figure (7) : The mean direction of the minimum stress σ3 was found 222°, while the mean direction of the maximum stress σ1 was 137° (this study).

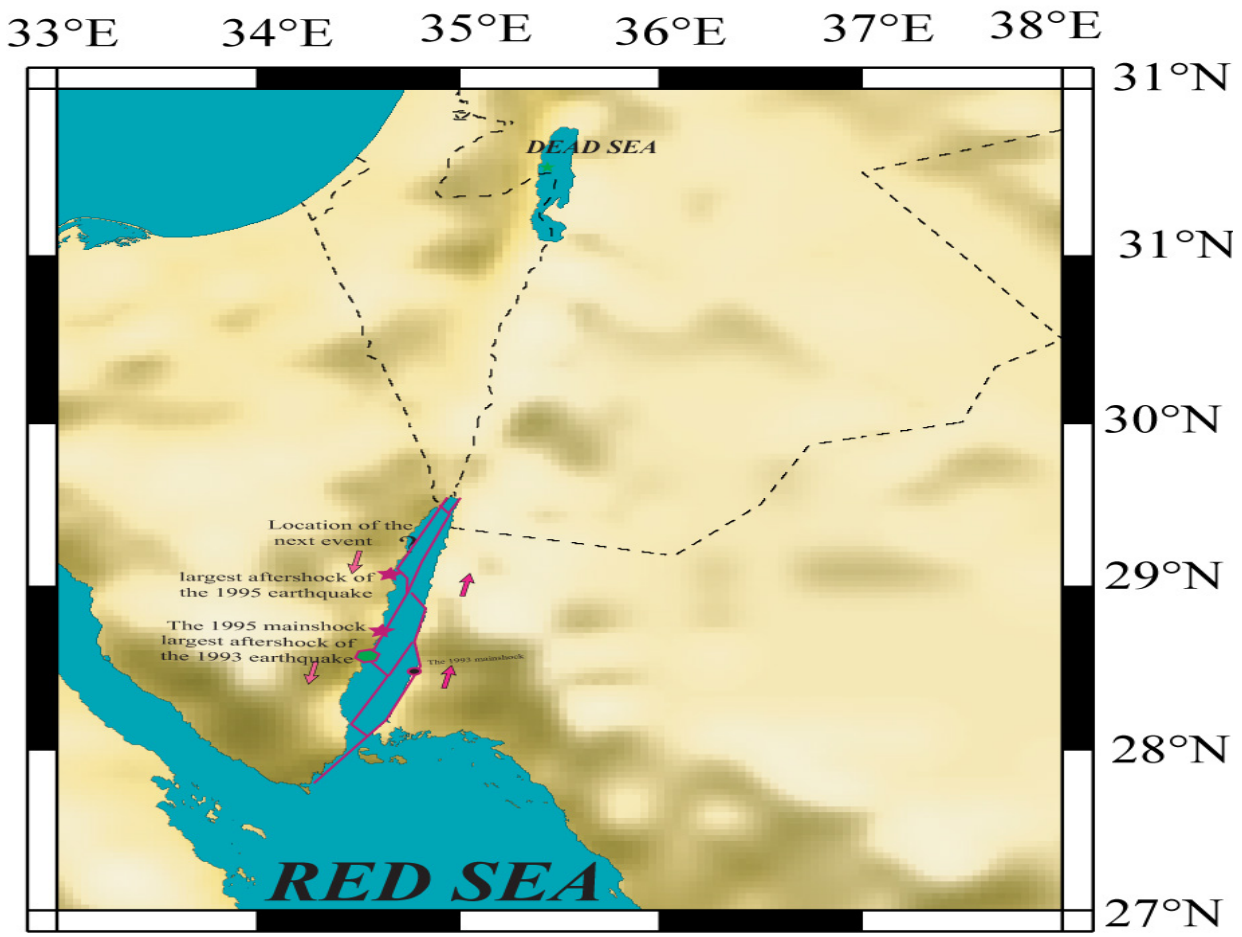

Figure 8 Generalized model for the migration of large earthquakes in the Gulf of Aqaba.

TECTONIC STRESS

First motion focal mechanisms were obtained for fifty-four earthquakes for the period 1985 to 1993, including the 1995 main-shock focal mechanism. The data were specially scrutinised for reverse instrument polarities. The earthquakes were clustered along and near by the Gulf of Aqaba. The alignment of the lineaments and the epicentres strongly suggest a considerable degree of correlation for the events that their focal mechanisms were obtained. 21% shows left-lateral strike slip fault mechanisms. 73% shows a component of a strike-slip fault movement (49% normal with some component of a strike-slip fault), while the remainder show pure normal and reverse fault mechanisms (4% normal).

Most of these solutions indicate that the NE striking Dead Sea-Gulf of Aqaba transform is still undergoing movement and this agrees with most recent motion on the surface faults of the Dead Sea-Gulf of Aqaba fault system.

The state of stress in the Gulf of Aqaba and the Dead Sea Transform (Northwest of the study area) appears to be characterized by Northeast-Southwest extension, as indicated by the focal mechanisms (Al-Amri, 1990), which is shown in Figure 6, and by a fault orientation analysis (Reches, 1987). The tectonic stress field is characterized by Northeast-Southwest extensional stress, as indicated by focal mechanisms with T-axes generally aligned Northeast-Southwest.

Al-Amri (1990) found that the maximum compressive stress ($\sigma 1$) orientation in the range of N 15° W to N 47° W and the minimum compressive stress ($\sigma 3$) orientation in the range between N 42° E to N 90° E.

The mean direction of the minimum stress $\sigma 3$ was found 222°, while the mean direction of the maximum stress $\sigma 1$ was 137° (Figure 7). All these seismic measurements are in good agreement with the geologically inferred principal stress directions for the region by Reches (1987). He indicates that the Dead Sea Transform is discontinuous and includes more than 10

pull-apart basins and a few push-up swells. His model in figure 6b is based on the following characteristics:

a) Left lateral displacement of about 105 km has occurred along the Dead Sea Transform since the Middle Miocene;

b) The deformation along the Dead Sea Transform and the minor extension normal to it;

c) The stress field that exists along the transform can be represented by stress determined from small scale structures by Eyal and Reches (1983).

All these studies and this work indicate north-northwest-trending, maximum compressive stress ($\sigma 1$) and northeast-trending, near-horizontal minimum compressive stress ($\sigma 3$).

DISCUSSION

It has been observed in many cases that the mainshock epicenters were very often located at one end of the aftershock zone (Matsuzawa, 1979). In the Gulf of Aqaba this happens with the 1993 and 1995 sequences, where the mainshock of the 1993 was located at the south end of the aftershock zone and below the bottom depth of the aftershock zone. This is also applied to the 1995 sequence where the mainshock is located near the south end of the aftershock zone at a depth representing the bottom of the aftershock zone. For both sequences most aftershocks concentrate between the mainshock and the largest aftershock (Figure 3a and 3b).

The characteristics of aftershocks give clues about the nature of the relatively long term processes that redistribute stress following the more or less instantaneous stress change associated with the mainshock (Wesson, 1987). It seems likely that these same processes are responsible for the concentration of stress in the hypocentral region of the largest 1993 aftershocks prior to and resulting in the nucleation of the 1995 mainshock. This systematic northward migration leads one to suggest an initial model for the earthquake migration in the Gulf of Aqaba (Figure 8), although the real migration is likely to be more complicated. However, shortly, in this model the epicenter of the largest aftershock represents the area of stresses nucleation and location of next large mainshock (Figure 8).

CONCLUSION

A possible mechanism of earthquakes in the Gulf of Aqaba fault system is proposed that seismic energies are accumulated gradually till reaching a failure point. At that time a large stress drop during a mainshock (the 1993 mainshock), which caused redistribute of stresses to the location of the largest aftershock which trigger the area to be an area of stress nucleation that generate another large mainshock (the 1995 earthquake). Again the area of the largest aftershock of last mainshock could receive next large mainshock. Because a future large earthquake could easily nucleate in the Gulf of Aqaba, more effort is needed to fully understand the stress migration and seismic behavior a long this critical section of the southern Dead Sea faults system.

REFERENCES

Al-Amri, A. M., 1990. An Investigation of the seismicity and the aeromagnetic features of the structural framework in the Gulf of Aqaba and the adjoining land region, Midyan, Northern Red Sea, Ph.D. Thesis, University of Minnesota, USA, 251 p.

Al-Arifi, N. S., 1996. Micro-seismicity and lineament study of the eastern side of the Gulf of Aqaba NW Saudi Arabia (1986-1994), Ph.D. Thesis, University of Manchester, UK, 492p.

Al-Shaabi, S., 1998. The seismicity of the Gulf of Aqaba, Northern Red Sea (1985-1995), M.Sc. Thesis, University of Leeds, UK, 148p.

Ben-Avraham, Z., Garfunkel, Z., Almagor, G., and Hall, J. K., 1979. Continental break-up by leaky transform; the Gulf of Elat (Aqaba), Science (AAAS)206:4415, pp. 214-216.

Freund, R., Garfunkel, Z. , Zak, I., Goldberg, M., Weissbord, T., and Devin, B., 1970. The shear along the Dead Sea rift, Philos. Trans. of the Royal Society of London, Series A, Volume 267, pp. 107-130.

El-Isa, Z., H. Merghelani and M. Bazzari, 1984. The Gulf of Aqaba earthquake swarm of 1983, January-April, *Geophysical Journal of the Royal Astronomical Society*, Volume 78, pp. 711-722.

Hall, J. and Ben-Avraham, Z., 1978. New bathymetric map of the Gulf of Eilat (Aqaba), Tenth International Congress on Sedimentology, Abstract, 1:285, Scale 1:250000.

Quennell, A. M., 1958. The structural and geomorphic evolution of the Dead Sea rift. Quarterly Journal of the Geological Society of London, Volume 114, pp. 1-24.

Quennell, A. M., 1959. Tectonics of the Dead Sea rift. Proc. 20th inter. Geolog. Congr., Mexico, pp. 385-403.

Reches, Z., 1987. Mechanical aspects of pull-apart basin and push-up swells with applications to the Dead Sea Transform. Tectonophysics, Volume 141, pp. 75-88.

Reiss, Z. and Hottinger, L., 1984. The Gulf of Aqaba: Ecological Micropaleontology, Ecological studies, Volume 50, 330p. Springe-Verlag.